

New upper bound on the scattering cross section of slow neutrons on liquid parahydrogen from neutron transmission

K. B. Grammer,^{1,*} R. Alarcon,² L. Barrón-Palos,³ D. Blyth,² J. D. Bowman,⁴ J. Calarco,⁵ C. Crawford,⁶ K. Craycraft,^{1,6} D. Evans,⁷ N. Fomin,¹ J. Fry,⁸ M. Gericke,⁹ R. C. Gillis,⁸ G. L. Greene,^{1,4} J. Hamblen,¹⁰ C. Hayes,¹ S. Kucuker,¹ R. Mahurin,^{11,9} M. Maldonado-Velázquez,³ E. Martin,⁶ M. McCrea,⁹ P. E. Mueller,⁴ M. Musgrave,¹ H. Nann,⁸ S. I. Penttilä,⁴ W. M. Snow,⁸ Z. Tang,^{12,8} and W. S. Wilburn¹²

¹*University of Tennessee, Knoxville, TN, USA*

²*Arizona State University, Tempe, AZ, USA*

³*Universidad Nacional Autónoma de México, Mexico, DF, Mexico*

⁴*Oak Ridge National Lab, Oak Ridge, TN, USA*

⁵*University of New Hampshire, Durham, NH, USA*

⁶*University of Kentucky, Lexington, KY, USA*

⁷*University of Virginia, Charlottesville, VA, USA*

⁸*Indiana University, Bloomington, IN, USA*

⁹*University of Manitoba, Winnipeg, Canada*

¹⁰*University of Tennessee-Chattanooga, Chattanooga, TN, USA*

¹¹*Middle Tennessee State University, Murfreesboro, TN, USA*

¹²*Los Alamos National Laboratory, Los Alamos, NM, USA*

(Dated: December 7, 2024)

The scattering of slow neutron beams provides unique, non-destructive, quantitative information on the structure and dynamics of materials of interest in physics, chemistry, materials science, biology, geology, and other fields. Liquid hydrogen is a widely-used neutron moderator medium, and an accurate knowledge of its slow neutron cross section is essential for the design and optimization of intense slow neutron sources. In particular the rapid drop of the slow neutron scattering cross section of liquid parahydrogen below 15 meV, which renders the moderator volume transparent to the neutron energies of most interest for scattering studies, is therefore especially interesting and important. We have placed an upper bound on the total cross section and the scattering cross section for slow neutrons with energies between 0.43 meV and 16.1 meV on liquid hydrogen at 15.6 K using neutron transmission measurements on the hydrogen target of the NPDGamma collaboration at the Spallation Neutron Source at Oak Ridge National Laboratory. At 1 meV this new upper bound is a factor of 3 below the data from previous work which has been used in the design of liquid hydrogen moderators at slow neutron sources. We describe our measurements, compare them with previous work, and discuss the implications for designing more intense slow neutron sources.

PACS numbers: 28.20.Cz, 28.20.Ka, 28.20.Gd

The successful development of intense slow neutron sources combined with the increasing phase space acceptance of neutron optical components has enabled a dramatic expansion of the scientific applications of neutron scattering to encompass many fields in science and technology. The broad applicability of the non-destructive, quantitative information that slow neutron scattering can provide on the internal structure and dynamics of condensed media has motivated the construction of several new neutron scattering facilities over the last decade. The efficiency of the moderating medium which accepts the relatively high energy neutrons liberated from the nucleus and cools them to the slow neutron energy range below 25 meV determines the phase space density of the neutron beams. New results on physics relevant to the moderation process are therefore of interest to a very broad range of the scientific community.

Many intense neutron sources use liquid hydrogen as a neutron moderator medium. The near-equality of the neutron and proton mass coupled with the anomalously large s-wave neutron-proton scattering amplitude allow

a hydrogen-rich medium to both efficiently lower the incident neutron energy through collisions and also maintain a small neutron mean free path to keep the neutron phase space density high at the source. In the slow neutron regime, however, the neutron scattering cross section and therefore the mean free path is sensitive to the interference of the scattering amplitudes from neighboring atoms.

In this context, neutron scattering from molecular hydrogen is especially interesting. Molecular hydrogen has two spin states, labeled orthohydrogen ($J = \text{odd}$) and parahydrogen ($J = \text{even}$). The lowest orthohydrogen state ($J = 1$) lies 15 meV above the lowest parahydrogen state ($J = 0$). The spin singlet state of the protons in the parahydrogen molecule combined with the measured spin dependence of s-wave neutron-proton scattering amplitudes conspire to greatly suppress the total scattering cross section for neutrons on parahydrogen molecules by more than one order of magnitude relative to that from the hydrogen atom. The total scattering cross section on orthohydrogen is approximately 50 times higher than

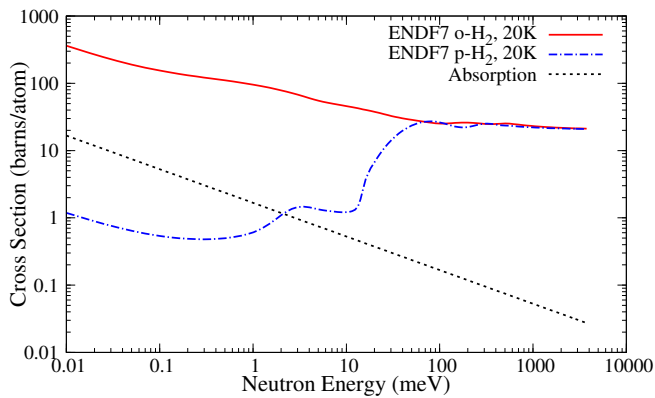


FIG. 1. Parahydrogen and orthohydrogen scattering cross sections at 20 K from ENDF-VII [1] and the absorption cross section [2].

on parahydrogen (Fig. 1) because the destructive interference between the atoms is absent. Furthermore, this scattering cross section decrease happens for slow neutron energies below the 15 meV energy threshold for the neutron spin flip scattering process which turns parahydrogen into orthohydrogen. The moderator therefore becomes transparent to the neutrons just as they enter the slow neutron energy range of interest for neutron scattering applications. Consequently, many studies have shown that the slow neutron intensity from a liquid hydrogen moderator can be greatly increased if the molecules are maintained in the parahydrogen molecular state [3][4][5]. Therefore, the transmission of neutrons through liquid hydrogen is acutely sensitive to the relative concentrations of orthohydrogen and parahydrogen.

In this work, we show that this decrease of the total scattering cross section in liquid parahydrogen in the slow neutron regime is much more rapid than previously realized. We draw this conclusion from a comparison of our measured upper bound on the total cross section for neutrons with energies between 0.43 meV to 16.1 meV in liquid hydrogen at a temperature of $15.6 \text{ K} \pm 0.6 \text{ K}$ with previous data [6][7][8]. This measurement was conducted at the Spallation Neutron Source (SNS) at Oak Ridge National Laboratory using a 16-liter liquid hydrogen target [9] operated on the Fundamental Neutron Physics Beamline [10] (FnPB) by the NPDGamma collaboration.

Figure 2 shows the experimental setup for the transmission measurement on the FnPB beamline at the SNS. The cross sectional area of the neutron beam is $12 \times 10 \text{ cm}^2$ at the exit of the neutron guide. Neutrons then pass through the normalization monitor, a multi-wire proportional counter [11] with a gas mixture of ^3He (15.1 Torr) and N_2 (750 Torr) located $15.24 \text{ m} \pm 0.12 \text{ m}$ from the moderator. Neutrons are polarized using a supermirror polarizer [12]; however, the direction of the polarization is reversed at 60 Hz by a spin rotator and pulse averaging analysis results in an effectively unpolar-

ized beam. Neutrons are incident on the 16 liter liquid hydrogen target [9] centered 17.6 m from the moderator. Roughly 60% of the neutron beam is captured on the hydrogen in the target with the 2.2 MeV capture gammas relevant to the NPDGamma experiment detected by 48 cesium iodide crystals. The effective length of liquid hydrogen covered by the neutron beam cross sectional area including beam divergence is $30.065 \text{ cm} \pm 0.005 \text{ cm}$ when cold. The transmitted neutrons exit the downstream end of the target vessel through a 2.5 cm diameter aperture in the ^6Li -rich neutron absorber surrounding the target. The transmitted neutron intensity is measured in a ^3He plate ion chamber [13] located $3.44 \text{ m} \pm 0.12 \text{ m}$ from the normalization monitor. The charge produced in the monitors is amplified by current-voltage amplifiers [14] with a 10 kHz bandwidth.

The data acquisition system records data in 0.4 ms increments. In order to avoid contamination from overlapping neutron pulses and to increase the dynamic range of neutron energies for the transmission measurement, data were taken with the two beamline choppers parked open while the SNS was operating at 10 Hz duty cycle rather than the normal 60 Hz.

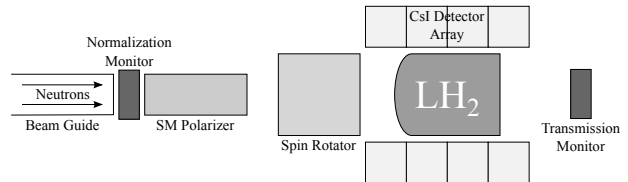


FIG. 2. Experimental setup showing the cesium iodide detector array, liquid hydrogen target, beam monitors, polarizer, and spin rotator.

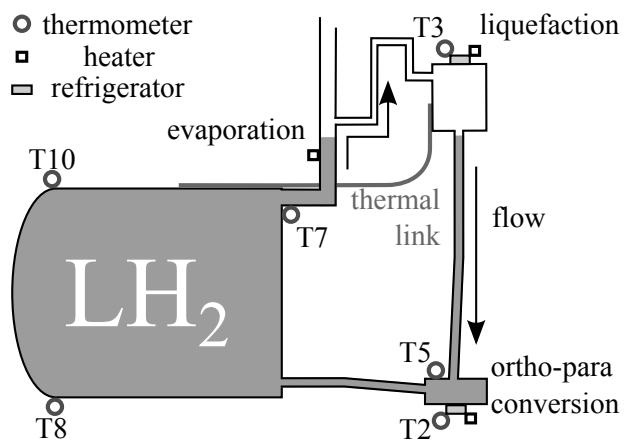


FIG. 3. Diagram of circulation loop inside the hydrogen target system. Evaporated hydrogen is re-condensed and is forced to flow through the ortho-para convertor (OPC) at a rate of a few millimoles per second. T3, T7, T8, and T10 determine the liquid hydrogen bulk temperature. T2 and T5 determine the temperature of the catalyst in the OPC.

The target vessel is initially filled with hydrogen gas with 3 orthohydrogen molecules per parahydrogen molecule from equipartition. The equilibrium parahydrogen concentration increases with decreasing temperature [15]. The slow natural conversion to parahydrogen is accelerated by circulation of the liquid through 150 mL of hydrous iron (III) oxide [16] 30 - 50 mesh powder catalyst in the ortho-para converter (OPC) [17] in the NPDGamma target loop (Fig. 3). The neutron transmission increases with time as hydrogen circulates through the catalyst until a steady-state condition is reached. Fitting the transmission for 3.42 meV neutrons to an exponential as a function of time (Fig. 4) indicates that the parahydrogen concentration in the main target vessel approaches saturation. This exponential approach to the steady-state condition implies that the conversion is dominated by the first order processes in the OPC as liquid hydrogen circulates through the catalyst.

The conversion process shown in figure 4 has reached steady-state, where the parahydrogen concentration is near the thermal equilibrium value defined by the temperature of the OPC. The average temperature of the OPC was $15.4 \text{ K} \pm 0.5 \text{ K}$, which corresponds to a thermal equilibrium parahydrogen concentration of 0.99985. A small amount of para-to-ortho conversion may take place in the liquid in the main vessel, on the walls of the vessel, or the walls of the circulation loop that prevents reaching absolute thermal equilibrium. Since para-to-ortho conversion is known to be a very slow process it is not expected to limit the ortho-para ratio in the liquid hydrogen, and the liquid hydrogen is expected to be in thermal equilibrium with the catalyst. However, it was not possible to independently confirm the parahydrogen concentration in this system.

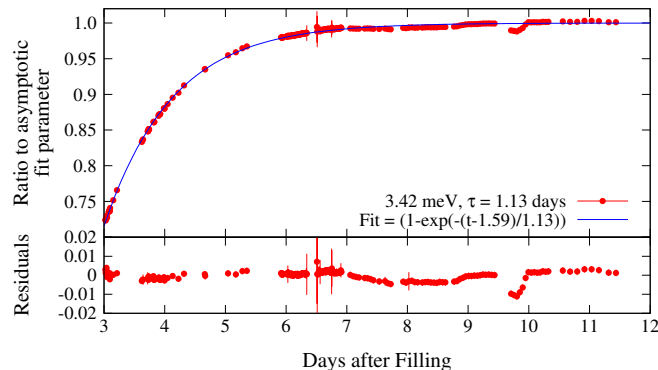


FIG. 4. Observed ortho-para conversion over time as a fraction of the asymptotic limit for 3.42 meV neutrons shortly after filling the target, with a time constant of approximately 1 day. Residuals from the exponential fit are shown at bottom.

Two different measurements were required in order to measure the empty target and full target transmissions. The full target measurement was performed over 8 hours

with the target vessel at 15.6 K after the target had been in steady-state operation for 4 weeks, which corresponds to 30 conversion time constants. The empty target measurement was performed 2 weeks later with the target vessel at 16.3 K in order to cancel the temperature dependence of scattering from the aluminum target vessel. Between these two measurements, the beamline moderator was emptied and refilled with fresh liquid hydrogen, which led to a small change in the moderated neutron spectrum between the two measurements. A neutron energy dependent correction was applied to the transmission monitor signals using the ratio of the normalization monitor signals to account for this systematic effect. For each neutron pulse, the signals in each monitor are normalized to the per-pulse beam power by integrating the normalization monitor over peak signal range.

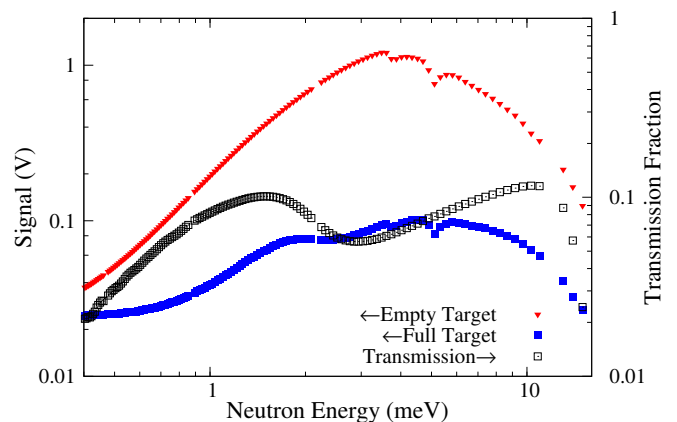


FIG. 5. Transmission monitor signals (left axis) for empty (red) and hydrogen-filled (blue) aluminum target vessel. Dips in the spectra are at the aluminum Bragg edges. Transmission ratio (right axis, black) depicts no transmission for energies above 14.5 meV spin-flip transition.

There is not a direct correspondence between time of flight bins in each monitor due to time of flight broadening. The normalization monitor signal is fit to a cubic spline in order to interpolate for spectrum normalization. The sharp dips in the pulse shapes in figure 5 are due to Bragg scattering on aluminum windows along the path of the neutron beam. These dips are visible at neutron energies of 4.98 meV and 3.74 meV, corresponding to the aluminum (200) and (111) Bragg planes [18], respectively. The time of flight of the Bragg edges for the normalization monitor is used to determine the distance from the moderator and to convert each time of flight bin to a neutron energy. The target-full spectrum indicates no measurable neutron flux for energies above 14.5 meV (Fig. 5). This is the minimum energy necessary for the $J = 0 \rightarrow 1$ spin-flip transition, meaning neutrons with energies above this threshold are scattered out of the beam rather than transmitted through the target. The data also contain a 240 Hz noise component with an am-

plitude of a few millivolts. The amplitude is diminished by averaging pulses over the measurement period and is only visible for small signals. The transmission monitor signals at long wavelengths are fit to a sinusoidal function corresponding to the 240 Hz noise. The sinusoidal function is subtracted before extracting the transmission. After correcting for the pedestal, 240 Hz noise, and moderator spectrum, the final corrected transmission (Fig. 5) is given by

$$T(\lambda) = \frac{S_{\text{trans,full}}(\lambda)}{S_{\text{trans,empty}}(\lambda)} \frac{S_{\text{norm,empty}}(\lambda)}{S_{\text{norm,full}}(\lambda)} \frac{g_{\text{norm}}}{g_{\text{trans}}}, \quad (1)$$

where the S values are monitor signals and g are monitor gain adjustment factors.

The contamination of the transmission signal by non-forward small angle scattering of neutrons in our geometry was estimated to be less than 0.1% in MCNPX [19] using the ENDF-VII thermal cross sections [1]. The total cross section can then be written as:

$$\begin{aligned} \sigma_{\text{total}}(\lambda) &= \frac{-\log[T(\lambda)]}{nl} \\ &= \sigma_{\text{abs}}(\lambda) + \sigma_{\text{scatter}}(\lambda) \\ &= \sigma_{\text{abs}}(\lambda) + f \times \sigma_{\text{para}} + (1-f)\sigma_{\text{ortho}}, \end{aligned} \quad (2)$$

where n is the number density, l is the hydrogen length, f is the parahydrogen fraction, $\sigma_{\text{abs}} = 0.3326 \pm 0.0007$ barns at 2200m/s [2], σ_{scatter} is the total scattering cross section, σ_{ortho} is the orthohydrogen scattering cross section, and σ_{para} is the parahydrogen scattering cross section.

The diode temperature sensors have an accuracy of 0.5 K and upward drift due to radiation damage is not worse than 0.3 K, providing a total uncertainty on the temperature of 0.6 K. The density of the liquid hydrogen in our target is determined from a fit to data compilations of the density of liquid hydrogen as a function of temperature from many sources [20][21][22]. The transmission data include several instrumental effects such as the monitor efficiency, the monitor dead layer, and monitor linearity. These effects all cancel in the expression above as long as the monitors and preamplifiers are linear and the aluminum components of the experiment were maintained at the same temperature. The linearity of the transmission monitor was determined from a scan of the bias voltage in order to reduce volume recombination effects in the chambers, with a resulting uncertainty of 0.15% for each monitor. Controlled current injection was used to measure the linearity of preamplifiers and the gain shift, which are 0.01% and 0.1% respectively.

We have determined the upper limit on the total cross section for liquid hydrogen at 15.6 K from approximately 0.43 meV to 16.1 meV with an uncertainty of approximately 1%, or 0.02 barn/atom over the majority of

TABLE I. Main uncertainties in the total cross section at 1.92 meV

Source	Uncertainty
Neutrons	0.02%
Monitor Position	0.61%
Monitor Gains	0.06%
Monitor Linearity	0.12%
Target Length	0.007%
Liquid Density Fit	0.5%
Temperature	0.71%
Total	1.07%

the measurement range (Fig. 6). Because the absorption cross section is well known, we are also able to set an upper limit on the parahydrogen scattering cross section at these energies. This upper bound is much smaller than the values previously reported in the literature [6][7][8] (Fig. 7).

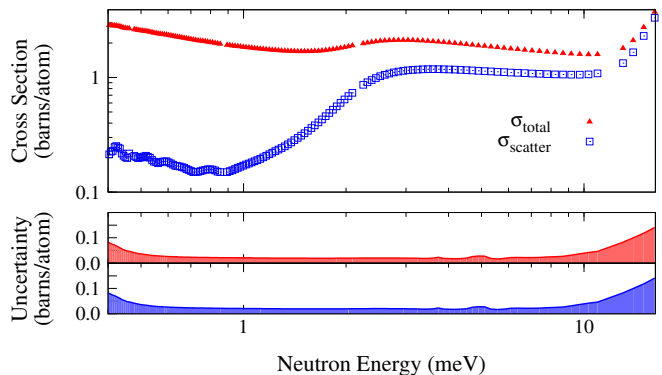


FIG. 6. Upper limit on the total cross section from this work in barns/atom (red triangles, top), upper limit on the parahydrogen cross section (blue squares, bottom). Shaded plots are total uncertainty (systematic and statistical).

The measurement of the parahydrogen scattering cross section is very sensitive to the orthohydrogen fraction in the target volume because the orthohydrogen cross section is approximately a factor of 50 greater than for parahydrogen. The upper limit on the parahydrogen scattering cross section from this work along with the Seiffert [6] data and the ENDF-VII parahydrogen kernel evaluated at 20 K [1] are compared in Fig. 7. The significant difference in magnitude suggests the presence of unaccounted for orthohydrogen contamination in the Seiffert sample. Subtraction of an admixture of 0.5% orthohydrogen from Seiffert data brings both results into agreement.

The Squires measurement [7] was performed using a gas mixture with a parahydrogen concentration of 0.9979, which was independently measured using thermal conductivity. The Seiffert [6] and Celli [8] measurements

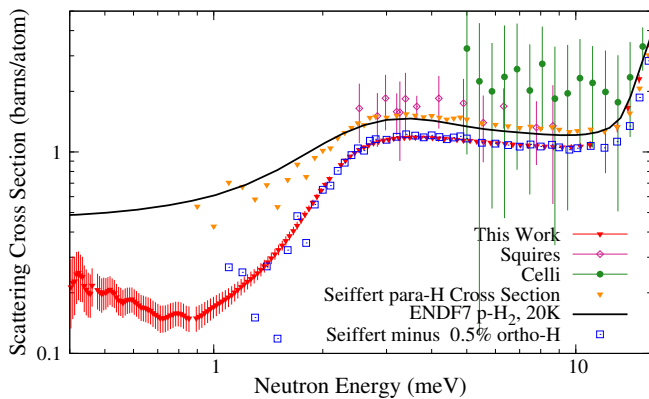


FIG. 7. The scattering cross section extracted in this work (red), Squires [7] (magenta), Celli [8] (green, some points omitted), Seiffert [6] (orange), ENDF-VII (black), and subtraction of a 0.5% admixture of orthohydrogen from Seiffert (blue).

were both performed using liquid hydrogen in the presence of a catalyst; however, neither experiment independently determined the orthohydrogen concentration but rather inferred that it was either negligible, in the case of Seiffert, or at thermal equilibrium, in the case of Celli. We therefore treat both the Seiffert and Celli measurements as upper limits as we do for our data. We conclude that our target system must have less orthohydrogen contamination than these previous two measurements because our observed total cross section is lower. Of these three measurements in the literature and the measurement in this work, we believe that our measurement has the lowest orthohydrogen contamination and that it provides the most accurate upper limit on the liquid parahydrogen scattering cross section.

These results have important implications for the design of slow neutron sources. They imply that the intensity of neutron moderators based on liquid hydrogen can be increased if the liquid can be maintained in the parahydrogen molecular state. Recent simulation work conducted for the European Spallation Source project [4], indicates increased source intensity from liquid parahydrogen neutron moderators incorporated into a realistic target-moderator geometry. Measurements at J-PARC [3] and LANSCE [5] also show that the moderator intensity for neutrons below 15 meV are highly dependent on the ortho/para ratio. Our work shows that the parahydrogen cross section is overestimated throughout the slow neutron regime of interest. This overestimate reaches a factor of 3 at a neutron energy of 1 meV. The potential for increased slow neutron source intensity from liquid parahydrogen moderators is therefore greater than previously realized. In order to be able to take full advantage of this potential, however, it would be necessary to maintain the liquid in the parahydrogen state in the presence of the intense radiation environment which in-

evitably accompanies a intense neutron source [23]. Liquid hydrogen target designs which employ active circulation of the hydrogen through a catalyst coupled with dedicated measurements of the parahydrogen fraction from a liquid hydrogen moderator operated in an intense radiation environment are needed to confirm this potential and demonstrate that it can be realized at an intense neutron source.

We would like to thank Erik Iverson, Phillip Ferguson, Kenneth Herwig, and Franz Gallmeier for productive discussions and encouragement for this experiment. We thank the management and staff of the Spallation Neutron Source for adapting our measurement to the busy beam delivery schedule. We gratefully acknowledge the support of the U.S. Department of Energy Office of Nuclear Physics (including Grant No. DE-FG02-03ER41258), the National Science Foundation (including Grant No. PHY-1068712), PAPIIT-UNAM (Grant No. IN111913), and the Indiana University Center for Space-time Symmetries.

* kgrammer@vols.utk.edu

- [1] M. B. Chadwick *et al.*, Nucl. Data Sheets **112**, 2887 (2011).
- [2] S. F. Mughabghab, “Atlas of Neutron Resonances, 5-th ed,” (2006).
- [3] T. Kai, M. Harada, M. Teshigawara, N. Watanabe, and Y. Ikeda, Nucl. Instruments Methods Phys. Res. Sect. A Accel. Spectrometers, Detect. Assoc. Equip. **523**, 398 (2004).
- [4] M. Magán *et al.*, Nucl. Instruments Methods Phys. Res. Sect. A Accel. Spectrometers, Detect. Assoc. Equip. **729**, 417 (2013).
- [5] M. Ooi *et al.*, Nucl. Instruments Methods Phys. Res. Sect. A Accel. Spectrometers, Detect. Assoc. Equip. **566**, 699 (2006).
- [6] W. D. Seiffert, B. Weckermann, and R. Misenta, Z. Naturforsch. Tl. A **25**, 967 (1970).
- [7] G. L. Squires and A. T. Stewart, Proc. R. Soc. A Math. Phys. Eng. Sci. **230**, 19 (1955).
- [8] M. Celli, N. Rhodes, A. K. Soper, and M. Zoppi, J. Phys. Condens. Matter **11**, 10229 (1999).
- [9] S. Santra *et al.*, Nucl. Instruments Methods Phys. Res. Sect. A Accel. Spectrometers, Detect. Assoc. Equip. **620**, 421 (2010).
- [10] N. Fomin, “Fundamental neutron physics beamline,” In preparation.
- [11] M. McCrea, Private Communication (2012).
- [12] S. Balascuta *et al.*, Nucl. Instruments Methods Phys. Res. Sect. A Accel. Spectrometers, Detect. Assoc. Equip. **671**, 137 (2012).
- [13] J. Szymanski *et al.*, Nucl. Instruments Methods Phys. Res. Sect. A Accel. Spectrometers, Detect. Assoc. Equip. **340**, 564 (1994).
- [14] Artifex Engineering, Dortmund Str. 16-18, 26723 Emden, Germany, “Flexible Transimpedance Amplifier,”.
- [15] D. M. Dennison, Proc. R. Soc. A Math. Phys. Eng. Sci. **115**, 483 (1927).

- [16] Sigma-Aldridge Corp., 3050 Spruce Street, St. Louis, MO 63103, USA, “Product Number 371254-250G.”
- [17] L. Barrón-Palos *et al.*, Nucl. Instruments Methods Phys. Res. Sect. A Accel. Spectrometers, Detect. Assoc. Equip. **659**, 579 (2011).
- [18] R. Wyckoff, *Crystal structures* (1963).
- [19] D. B. Pelowitz, “MCNPX User’s Manual,” (2011).
- [20] J. W. Leachman, R. T. Jacobsen, S. G. Penoncello, and E. W. Lemmon, J. Phys. Chem. Ref. Data **38**, 721 (2009).
- [21] P. Souers, *Hydrogen properties for fusion energy* (1986).
- [22] R. McCarty, J. Hord, and H. Roder, (1981).
- [23] E. Iverson and J. Carpenter, in *ICANS-XVI, Proc. Int. Collab. Adv. Neutron Sources, Neuss, Ger.*, edited by H. Conrad (2003) pp. 707—718.